2007 IEEE International Conference on
Robotics and Automation
Roma, Italy, 10-14 April 2007

A Pattern Generator of Humanoid Robots Walking on a Rough Terrain

Hirohisa Hirukawa, Shizuko Hattori, Shuuji Kajita, Kensuke Harada,
Kenji Kaneko, Fumio Kanehiro, Mitsuharu Morisawa and Shinichiro Nakaoka

***Abstract*— This paper presents a motion pattern generator of humanoid robots that walks on a flat plane, steps and a rough terrain. It is guaranteed rigorously that the desired contact between a humanoid robot and terrain should be maintained by keeping the contact wrench sum between them inside the contact wrench cone under the sufficient friction assumption. A walking pattern is generated by solving the contact wrench equations and by applying the resolved momentum control.**

I. INTRODUCTION

The ZMP (Zero Moment Point)[15] has been used as a stability criterion to judge if the contact between a foot of a legged robot and a floor should be kept while walking. It can judge the strong stability of a contact, where a contact is called strongly stable if it is guaranteed that the contact should be kept to a given external wrench[12]. A number of walking pattern generators have been proposed using the ZMP as the strong stability criterion (See [11], [10], [6] for example). But the ZMP is a rigorous stability criterion only when a robot walks on a flat plane without a contact between a hand and the environment under the sufficient friction assumption. When the ZMP is used to plan motion patterns of a robot that walks on a terrain other than a flat plane and/or a contact between a hand and the environment, some approximations should be introduced to judge the contact stability.

We have proposed a strong stability criterion that can judge if the contact between a robot and the environment should be kept rigorously under the sufficient friction assumption when the robot walks on an arbitrary terrain with a possible contact between a hand and the environment [5]. It was proved that the contact should be strongly stable if the contact wrench sum (CWS for short) is an internal element of the contact wrench cone (CWC for short), and that the CWS and CWC are equivalent to the ZMP and the supporting polygon respectively when the robot walks on a flat plane without a hand contact.

This paper presents a walking pattern generator using the CWS as the strong stability criterion, and so it is able to plan motion patterns of a humanoid robot that walks on an arbitrary terrain possibly with a contact between a hand and the terrain. It is guaranteed theoretically that the contact should be stable while walking under the sufficient friction assumption. The motion patterns are generated by solving the contact wrench equations and by applying the resolved momentum control[7].

This paper is organized as follows. Section 2 presents the details of the proposed pattern generator. Section 3 gives examples. Section 4 concludes the paper.

The authors are with Humanoid Robotics Group, Intelligent Systems Institute, National Institute of Advanced Industrial Science and Technology (AIST), 1-1-1- Umezono, Tsukuba, Japan hiro.hirukawa@aist.go.jp

II. PATTERN GENERATOR

A. Equations of Momentum

Let $p_B, \boldsymbol{v}_B, \boldsymbol{\omega}_B$ be the position, velocity and the angular velocity of the coordinates on the waist link of a humanoid robot respectively which is supposed to have six degrees of the freedom in the space with respect to the reference coordinates. Let n be the number of the joints connected to the link and $\dot{\boldsymbol{\theta}} : n \times 1$ the angular velocity of the joints. See Fig.1. Then the momentum of the robot $\mathcal{P}$ and the angular momentum about the center of the gravity $\mathcal{L}$ can be given by

$$\begin{bmatrix} \mathcal{P} \\ \mathcal{L} \end{bmatrix} = \begin{bmatrix} M\boldsymbol{E} & -M\hat{\boldsymbol{r}}_{B\to G} & \boldsymbol{M}_{\dot{\theta}} \\ \boldsymbol{0} & \tilde{\boldsymbol{I}} & \boldsymbol{H}_{\dot{\theta}} \end{bmatrix} \begin{bmatrix} \boldsymbol{v}_B \\ \boldsymbol{\omega}_B \\ \dot{\boldsymbol{\theta}} \end{bmatrix}, \quad (1)$$

where M is the total mass of the robot, $\boldsymbol{E}$ the 3×3 unit matrix, $\boldsymbol{r}_{B\to G}$ the position vector from the origin of the waist coordinates to the COG of the robot, $\tilde{\boldsymbol{I}} : 3 \times 3$ the inertia matrix about the COG, $\boldsymbol{M}_{\dot{\theta}} : 3 \times n$, $\boldsymbol{H}_{\dot{\theta}} : 3 \times n$ the inertia matrices which relate the joint velocities into the momentum and the angular momentum of the robot respectively. $\hat{}$ is the operator converting a 3×1 vector into a 3×3 skew-symmetric matrix whose multiplication from the left makes a vector product. Let x, y, z axes of the waist coordinates point to the front, left and top respectively.

Eq.(1) transforms $n+6$ velocity variables into 6 momentum variables, but in general the degrees of the freedom of the robot should degenerate because of the contact between the robot and the working environment. Let $\boldsymbol{v}_{F_i}, \boldsymbol{\omega}_{F_i}$ be the velocity and the angular velocity of the coordinates fixed at the i-th foot link ($i = 1, 2$), and $\boldsymbol{v}_{H_i}, \boldsymbol{\omega}_{H_i}$ those of the coordinates at the i-th hand link ($i = 1, 2$) respectively. $\boldsymbol{v}_{F_i}, \boldsymbol{\omega}_{F_i}$ and $\boldsymbol{v}_{H_i}, \boldsymbol{\omega}_{H_i}$ are constrained by the contact or by reference trajectories, and Eq.(1) under the constraints can be given by

$$\begin{bmatrix} \mathcal{P} \\ \mathcal{L} \end{bmatrix} = \begin{bmatrix} \boldsymbol{M}_B^* \\ \boldsymbol{H}_B^* \end{bmatrix} \boldsymbol{\xi}_B + \sum_{i=1}^{2} \{ \begin{bmatrix} \boldsymbol{M}_{F_i}^* \\ \boldsymbol{H}_{F_i}^* \end{bmatrix} \boldsymbol{\xi}_{F_i} + \begin{bmatrix} \boldsymbol{M}_{H_i}^* \\ \boldsymbol{H}_{H_i}^* \end{bmatrix} \boldsymbol{\xi}_{H_i} \}, \quad (2)$$

where

$$\boldsymbol{\xi}_B \equiv \begin{bmatrix} \boldsymbol{v}_B \\ \boldsymbol{\omega}_B \end{bmatrix}, \quad \boldsymbol{\xi}_{F_i} \equiv \begin{bmatrix} \boldsymbol{v}_{F_i} \\ \boldsymbol{\omega}_{F_i} \end{bmatrix}, \quad \boldsymbol{\xi}_{H_i} \equiv \begin{bmatrix} \boldsymbol{v}_{H_i} \\ \boldsymbol{\omega}_{H_i} \end{bmatrix},$$

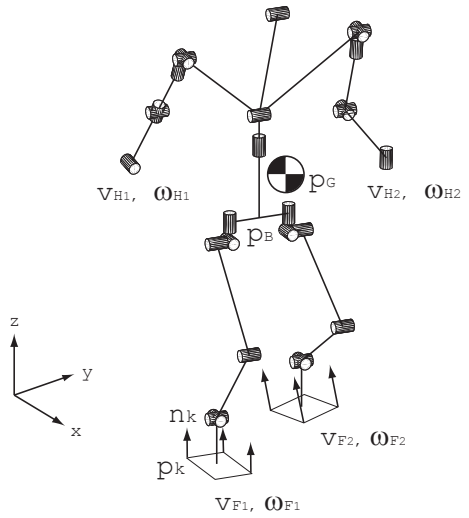

Fig. 1. Definitions of the coordinates

and $\boldsymbol{M}_B^*$, $\boldsymbol{H}_B^*$, $\boldsymbol{M}_{F_i}^*$, $\boldsymbol{H}_{F_i}^*$, $\boldsymbol{M}_{H_i}^*$, and $\boldsymbol{H}_{H_i}^*$ are the inertia matrices under the constraints and given by

$$\begin{aligned}
\begin{bmatrix} \boldsymbol{M}_B^* \\ \boldsymbol{H}_B^* \end{bmatrix} &\equiv \begin{bmatrix} M\boldsymbol{E} & -M\hat{\boldsymbol{r}}_{B\to G} \\ \boldsymbol{0} & \tilde{\boldsymbol{I}} \end{bmatrix} \\
&\quad - \sum_{i=1}^{2} \begin{bmatrix} \boldsymbol{M}_{F_i}^* \\ \boldsymbol{H}_{F_i}^* \end{bmatrix} \begin{bmatrix} \boldsymbol{E} & -\hat{\boldsymbol{r}}_{B\to F_i} \\ \boldsymbol{0} & \boldsymbol{E} \end{bmatrix} \\
&\quad - \sum_{i=1}^{2} \begin{bmatrix} \boldsymbol{M}_{H_i}^* \\ \boldsymbol{H}_{H_i}^* \end{bmatrix} \begin{bmatrix} \boldsymbol{E} & -\hat{\boldsymbol{r}}_{B\to H_i} \\ \boldsymbol{0} & \boldsymbol{E} \end{bmatrix}, \\
\begin{bmatrix} \boldsymbol{M}_{F_i}^* \\ \boldsymbol{H}_{F_i}^* \end{bmatrix} &\equiv \begin{bmatrix} \boldsymbol{M}_{leg_i} \\ \boldsymbol{H}_{leg_i} \end{bmatrix} \boldsymbol{J}_{leg_i}^{-1}, \\
\begin{bmatrix} \boldsymbol{M}_{H_i}^* \\ \boldsymbol{H}_{H_i}^* \end{bmatrix} &\equiv \begin{bmatrix} \boldsymbol{M}_{arm_i} \\ \boldsymbol{H}_{arm_i} \end{bmatrix} \boldsymbol{J}_{arm_i}^{-1},
\end{aligned}$$

where $\boldsymbol{J}_{leg_i}, \boldsymbol{J}_{arm_i}$ are 6×6 Jacobian matrices determined by the kinematics of the legs and arms, $\boldsymbol{r}_{B\to F_i}$ the position vector from the origin of the waist coordinates to the i-th foot coordinates, $\dot{\boldsymbol{\theta}}_{leg_i}(i = 1, 2)$ and $\dot{\boldsymbol{\theta}}_{arm_i}(i = 1, 2)$ 6×1 joint velocity vectors of the legs and the arms respectively, and the inertia matrices are decomposed into

$$\begin{aligned}
\dot{\boldsymbol{\theta}} &= [\dot{\boldsymbol{\theta}}_{leg_1}^T \quad \dot{\boldsymbol{\theta}}_{leg_2}^T \quad \dot{\boldsymbol{\theta}}_{arm_1}^T \quad \dot{\boldsymbol{\theta}}_{arm_2}^T]^T, \\
\boldsymbol{M}_{\dot{\theta}} &= [\boldsymbol{M}_{leg_1} \ \boldsymbol{M}_{leg_2} \ \boldsymbol{M}_{arm_1} \ \boldsymbol{M}_{arm_2}], \\
\boldsymbol{H}_{\dot{\theta}} &= [\boldsymbol{H}_{leg_1} \ \boldsymbol{H}_{leg_2} \ \boldsymbol{H}_{arm_1} \ \boldsymbol{H}_{arm_2}],
\end{aligned}$$

whose components correspond to two legs and two arms respectively [7].

B. Reference Angular Momentum

Since the reference of $\boldsymbol{v}_{F_i}, \boldsymbol{\omega}_{F_i}$ and $\boldsymbol{v}_{H_i}, \boldsymbol{\omega}_{H_i}$ are given, the joint velocity of the legs and the arms can be given by

$$\dot{\boldsymbol{\theta}}_{leg_i} = \boldsymbol{J}_{leg_i}^{-1} \begin{bmatrix} \boldsymbol{v}_{F_i} \\ \boldsymbol{\omega}_{F_i} \end{bmatrix} - \boldsymbol{J}_{leg_i}^{-1} \begin{bmatrix} \boldsymbol{E} & -\hat{\boldsymbol{r}}_{B\to F_i} \\ \boldsymbol{0} & \boldsymbol{E} \end{bmatrix} \begin{bmatrix} \boldsymbol{v}_B \\ \boldsymbol{\omega}_B \end{bmatrix}, \tag{3}$$

$$\dot{\boldsymbol{\theta}}_{arm_i} = \boldsymbol{J}_{arm_i}^{-1} \begin{bmatrix} \boldsymbol{v}_{H_i} \\ \boldsymbol{\omega}_{H_i} \end{bmatrix} - \boldsymbol{J}_{arm_i}^{-1} \begin{bmatrix} \boldsymbol{E} & -\hat{\boldsymbol{r}}_{B\to H_i} \\ \boldsymbol{0} & \boldsymbol{E} \end{bmatrix} \begin{bmatrix} \boldsymbol{v}_B \\ \boldsymbol{\omega}_B \end{bmatrix}, \tag{4}$$

from the reference of $(\boldsymbol{v}_B, \boldsymbol{\omega}_B)$, and then the reference of the angular momentum $\mathcal{L}^{ref}$ is found by Eq.(1). The reference of $\boldsymbol{v}_B$ is going to be tuned by solving the equations of the contact wrench in the following, but there is no criterion to design that of $\boldsymbol{\omega}_B$. One of the reasonable choices is to let $\boldsymbol{\omega}_B^{ref} = 0$ which should make the orientation of the waist link to be upright.

C. Equations of the Contact Wrench

Let the sum of the gravity and the inertia force applied to the robot be $\boldsymbol{f}_G$ and the sum of the moments about the COG of the robot $\boldsymbol{\tau}_G$ with respect to the reference coordinates, which can be given by

$$\begin{aligned}
\boldsymbol{f}_G &= M(\boldsymbol{g} - \ddot{\boldsymbol{p}}_G), &(5)\\
\boldsymbol{\tau}_G &= \boldsymbol{p}_G \times M(\boldsymbol{g} - \ddot{\boldsymbol{p}}_G) - \dot{\mathcal{L}}, &(6)
\end{aligned}$$

where $\boldsymbol{p}_G$ is the position vector of the COG with respect to the reference coordinates and $\boldsymbol{g} = [0 \ 0 \ -g]^T$ the gravity vector. Let us assume that sufficient friction exists at the contact. The assumption implies that an arbitrary friction force can be generated at every contact point with a positive normal force. Then the set of the contact wrench can be written by

$$\boldsymbol{f}_C = \sum_{k=1}^{K} \epsilon_k (\boldsymbol{n}_k + \sum_{l=1}^{2} \delta_k^l \boldsymbol{t}_k^l), \tag{7}$$

$$\boldsymbol{\tau}_C = \sum_{k=1}^{K} \boldsymbol{p}_k \times \epsilon_k (\boldsymbol{n}_k + \sum_{l=1}^{2} \delta_k^l \boldsymbol{t}_k^l), \tag{8}$$

where $\boldsymbol{n}_k$ is the unit normal vector at the k-th contact point $\boldsymbol{p}_k$, $\boldsymbol{t}_k^l (l = 1, 2)$ the unit tangent vectors at $\boldsymbol{p}_k$ whose linear combination spans the tangent plane at $\boldsymbol{p}_k$, ϵ_k a non-negative scalar, δ_k^l a scalar, and K the number of the contact points. See Fig.1 again. Let us call the set of the contact wrench *Contact Wrench Cone* or *CWC* for short, since the set forms a polyhedral convex cone. Then the strong contact stability can be determined as follows[5].

Theorem 1: **(Strong stability criterion)** If $(-\boldsymbol{f}_G, -\boldsymbol{\tau}_G)$ is an internal element of the CWC given by Eqs.(7) and (8), then the contact is strongly stable to $(\boldsymbol{f}_G, \boldsymbol{\tau}_G)$.

When $(-\boldsymbol{f}_G, -\boldsymbol{\tau}_G)$ is an internal element of the CWC, $(\boldsymbol{f}_G, \boldsymbol{\tau}_G)$ should balance with the sum of the contact wrench. We call the sum the *Contact Wrench Sum* or *CWS* for short. Then Theorem 1 can be rewritten as "If the CWS is an internal element of the CWC, then the contact is strongly stable to $(\boldsymbol{f}_G, \boldsymbol{\tau}_G)$". It was proved that this statement is equivalent to "If the ZMP is an internal element of the support polygon, then the contact is strongly stable, when the robot walks on a flat plane", and that the CWS is also a rigorous stability criterion in a generic case[5].

The pattern generators based on the ZMP criterion plan the reference trajectory of the ZMP, and then find the reference trajectory of the COG by solving the ZMP equations (see [6] for example). The proposed pattern generator plans the reference trajectory of the CWS, and then find the reference

trajectory of the COG by solving the equations of the contact wrench which can be derived by balancing the right hand sides of Eqs.(5) and (6) and those of Eqs.(7) and (8) respectively and given by

$$M\ddot{x}_G = \sum_{k=1}^{K}\epsilon_k n_{kx} + \sum_{k=1}^{K}\epsilon_k \sum_{l=1}^{2}\delta_k^l t_{kx}^l, \quad (9)$$

$$M\ddot{y}_G = \sum_{k=1}^{K}\epsilon_k n_{ky} + \sum_{k=1}^{K}\epsilon_k \sum_{l=1}^{2}\delta_k^l t_{ky}^l, \quad (10)$$

$$M(\ddot{z}_G + g) = \sum_{k=1}^{K}\epsilon_k n_{kz} + \sum_{k=1}^{K}\epsilon_k \sum_{l=1}^{2}\delta_k^l t_{kz}^l, \quad (11)$$

$$\begin{aligned} &M(\ddot{z}_G + g)y_G - M\ddot{y}_G z_G + \dot{\mathcal{L}}_x \\ &= \sum_{k=1}^{K}\epsilon_k(y_k n_{kz} - z_k n_{ky}) \\ &+ \sum_{k=1}^{K} y_k\epsilon_k \sum_{l=1}^{2}\delta_k^l t_{kz}^l - \sum_{k=1}^{K} z_k\epsilon_k \sum_{l=1}^{2}\delta_k^l t_{ky}^l, \end{aligned} \quad (12)$$

$$\begin{aligned} &-M(\ddot{z}_G + g)x_G + M\ddot{x}_G z_G + \dot{\mathcal{L}}_y \\ &= -\sum_{k=1}^{K}\epsilon_k(x_k n_{kz} - z_k n_{kx}) \\ &- \sum_{k=1}^{K} x_k\epsilon_k \sum_{l=1}^{2}\delta_k^l t_{kz}^l + \sum_{k=1}^{K} z_k\epsilon_k \sum_{l=1}^{2}\delta_k^l t_{kx}^l, \end{aligned} \quad (13)$$

$$\begin{aligned} &Mx_G\ddot{y}_G - My_G\ddot{x}_G + \dot{\mathcal{L}}_z \\ &= \sum_{k=1}^{K}\epsilon_k(x_k n_{ky} - y_k n_{kx}) \\ &+ \sum_{k=1}^{K} x_k\epsilon_k \sum_{l=1}^{2}\delta_k^l t_{ky}^l - \sum_{k=1}^{K} y_k\epsilon_k \sum_{l=1}^{2}\delta_k^l t_{kx}^l, \end{aligned} \quad (14)$$

where $\boldsymbol{p}_G = (x_G, y_G, z_G)$, $\boldsymbol{p}_k = (x_k, y_k, z_k)$, $\mathcal{L} = (\mathcal{L}_x, \mathcal{L}_y, \mathcal{L}_z)$, $\boldsymbol{n}_k = (n_{kx}, n_{ky}, n_{kz})$ and $\boldsymbol{t}_k^l = (t_{kx}^l, t_{ky}^l, t_{kz}^l)$.

The reference of the COG is planned based on the equations of the contact wrench as follows. At first, let us plan the reference of $\ddot{z}_G$. Then the force along the z-axis should balance as

$$M(\ddot{z}_G + g) = \sum_{k=1}^{K}\epsilon_k n_{kz} + \sum_{k=1}^{K}\epsilon_k \sum_{l=1}^{2}\delta_k^l t_{kz}^l, \quad (15)$$

in which the ratio between the first and second terms of the right hand side is arbitrary and we choose it as

$$\sum_{k=1}^{K}\epsilon_k n_{kz} = (1-\alpha)M(\ddot{z}_G + g), \quad (16)$$

$$\sum_{k=1}^{K}\epsilon_k \sum_{l=1}^{2}\delta_k^l t_{kz}^l = \alpha M(\ddot{z}_G + g), \quad (17)$$

where $\alpha = 1 - \frac{1}{K}\sum_{k=1}^{K} n_{kz}$. α has no rigorous physical meaning, but α can be considered as the average slope of the terrain.

Next ϵ_k should be chosen so that $0 < \epsilon_k$ holds for at least three k to keep the strong stability of Theorem 1. For example, the reference of ϵ_k can be chosen to be

$$\epsilon_k^{ref} = (1-\alpha)M(\ddot{z}_G + g)\frac{\lambda_k^{ref}}{\sum_{k=1}^{K}\lambda_k^{ref} n_{kz}}, \quad (18)$$

by using $0 < \lambda_k^{ref} \leq 1$ for three k at least. Then the reference trajectories of x_G, y_G are planned to follow the equations of the moments about the x and y axes

$$\begin{aligned} &M(\ddot{z}_G + g)(y_G - y_C) - M\ddot{y}_G(z_G - z_C) + \dot{\mathcal{L}}_x \\ &= \sum_{k=1}^{K}\epsilon_k(y_k n_{kz} - z_k n_{ky}) \equiv \tau'_{Cx}, \end{aligned} \quad (19)$$

$$\begin{aligned} &-M(\ddot{z}_G + g)(x_G - x_C) + M\ddot{x}_G(z_G - z_C) + \dot{\mathcal{L}}_y \\ &= -\sum_{k=1}^{K}\epsilon_k(x_k n_{kz} - z_k n_{kx}) \equiv \tau'_{Cy}, \end{aligned} \quad (20)$$

where y_C, z_C, x_C are defined by

$$y_C = \alpha\sum_{k=1}^{K}\frac{\epsilon_k}{\epsilon}y_k, \quad (21)$$

$$z_C = (1-\alpha)\sum_{k=1}^{K}\frac{\epsilon_k}{\epsilon}z_k, \quad (22)$$

$$x_C = \alpha\sum_{k=1}^{K}\frac{\epsilon_k}{\epsilon}x_k, \quad (23)$$

$$\epsilon = \sum_{k=1}^{K}\epsilon_k, \quad (24)$$

and $\tau'_{Cx(y)}$ is the moment about $x(y)$-axis excluding that from the friction force. The point $\boldsymbol{p}_C = (x_C, y_C, z_C)$ has no rigorous physical meaning, but $\boldsymbol{\tau}_C$ is not far from $\boldsymbol{p}_C \times \boldsymbol{f}_C$. Eqs.(19) and (20) are nonlinear differential equations, which can be solved by substituting a difference equation into $\ddot{x}_G$ and $\ddot{y}_G$ [10]. Then the friction forces have to satisfy equations

$$\begin{aligned} &\sum_{k=1}^{K} y_k\epsilon_k \sum_{l=1}^{2}\delta_k^l t_{kz}^l - \sum_{k=1}^{K} z_k\epsilon_k \sum_{l=1}^{2}\delta_k^l t_{ky}^l \\ &= -M(\ddot{z}_G + g)y_C + M\ddot{y}_G z_C, \end{aligned} \quad (25)$$

$$\begin{aligned} &-\sum_{k=1}^{K} x_k\epsilon_k \sum_{l=1}^{2}\delta_k^l t_{kz}^l + \sum_{k=1}^{K} z_k\epsilon_k \sum_{l=1}^{2}\delta_k^l t_{kx}^l \\ &= M(\ddot{z}_G + g)x_C - M\ddot{x}_G z_C. \end{aligned} \quad (26)$$

The selections of y_C, z_C, x_C are arbitrary, and the above definition implies that the friction force at each contact point should be proportional to the normal force at the point in the sense to satisfy Eqs.(21)-(26). Needless to say, it is not possible to control the friction force at each contact point in general. The friction forces should also satisfy Eqs.(9), (10)

and (14) which can be rewritten as

$$\sum_{k=1}^{K}\epsilon_k\sum_{l=1}^{2}\delta_k^l t_{kx}^l = M\ddot{x}_G - \sum_{k=1}^{K}\epsilon_k n_{kx}, \quad (27)$$

$$\sum_{k=1}^{K}\epsilon_k\sum_{l=1}^{2}\delta_k^l t_{ky}^l = M\ddot{y}_G - \sum_{k=1}^{K}\epsilon_k n_{ky}, \quad (28)$$

$$\sum_{k=1}^{K}x_k\epsilon_k\sum_{l=1}^{2}\delta_k^l t_{ky}^l - \sum_{k=1}^{K}y_k\epsilon_k\sum_{l=1}^{2}\delta_k^l t_{kx}^l = Mx_G\ddot{y}_G - My_G\ddot{x}_G + \dot{\mathcal{L}}_z - \sum_{k=1}^{K}\epsilon_k(x_k n_{ky} - y_k n_{kx}). \quad (29)$$

When $\ddot{z}_G^{ref}$ is given and $\ddot{x}_G^{ref}, \ddot{y}_G^{ref}$ are planned to follow Eqs.(19) and (20), it was turned out that the friction forces should satisfy Eqs.(27), (28), (17), (25), (26) and (29). At least six variables are necessary to satisfy the equations, which demands that $0 < \epsilon_k$ for three k at least. Without loss of the generality, let ϵ_k be positive for $k = 1, 2, 3$. Then the equations can be rewritten in a matrix form as

$$\begin{pmatrix} \epsilon_1\boldsymbol{t}_1^1 & \epsilon_1\boldsymbol{t}_1^2 & \cdots & \epsilon_3\boldsymbol{t}_3^1 & \epsilon_3\boldsymbol{t}_3^2 \\ \epsilon_1\boldsymbol{p}_1\times\boldsymbol{t}_1^1 & \epsilon_1\boldsymbol{p}_1\times\boldsymbol{t}_1^2 & \cdots & \epsilon_3\boldsymbol{p}_3\times\boldsymbol{t}_3^1 & \epsilon_3\boldsymbol{p}_3\times\boldsymbol{t}_3^2 \end{pmatrix} \begin{pmatrix} \delta_1^1 \\ \delta_1^2 \\ \vdots \\ \delta_3^1 \\ \delta_3^2 \end{pmatrix} = \begin{pmatrix} M\ddot{x}_G - \sum_{k=1}^{K}\epsilon_k n_{kx} \\ M\ddot{y}_G - \sum_{k=1}^{K}\epsilon_k n_{ky} \\ (1-\alpha)M(\ddot{z}_G + g) \\ -M(\ddot{z}_G + g)y_C + M\ddot{y}_G z_C \\ M(\ddot{z}_G + g)x_C - M\ddot{x}_G z_C \\ Mx_G\ddot{y}_G - My_G\ddot{x}_G + \dot{\mathcal{L}}_z - \sum_{k=1}^{K}\epsilon_k(x_k n_{ky} - y_k n_{kx}) \end{pmatrix}.$$

We call the linear equations the *Friction Force Equations* and it should have the unique solution if the 6×6 coefficient matrix in the left hand side is regular which is true if $\boldsymbol{p}_1, \boldsymbol{p}_2, \boldsymbol{p}_3$ are in a general position for example. Then there is a feasible reference for the friction forces, and therefore the generated pattern is also feasible.

Besides, the reference of the CWS is an internal element of the CWC, since ϵ_ks have been chosen to let the CWS of the normal forces be an internal element of the corresponding CWC. Note that the total CWS should be an internal element of the total CWC when the normal CWS is inside the normal CWC and the friction CWS inside the friction CWC, since the friction CWC forms linear subspaces and then the total CWC is the direct product of the normal CWC and the friction CWC[2].

When the number of the contact points with non-zero normal forces are more than three, the friction forces are indeterminate but there is a feasible solution if the friction force equations has a solution and it is not required to find the friction forces to generate the walking patterns.

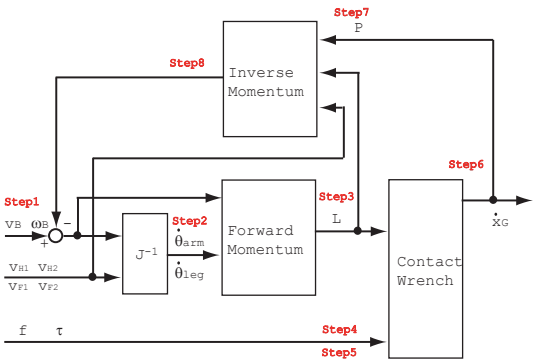

Fig. 2. Block diagram of the proposed pattern generator

D. Resolved Momentum Control

Let the solution of the equations of Eqs.(19) and (20) be (x_G^{ref}, y_G^{ref}), the reference of the momentum $(\mathcal{P}_x^{ref}, \mathcal{P}_y^{ref}, \mathcal{P}_z^{ref})$ can be given by

$$\mathcal{P}_x^{ref} = M\dot{x}_G^{ref}, \quad (30)$$

$$\mathcal{P}_y^{ref} = M\dot{y}_G^{ref}, \quad (31)$$

$$\mathcal{P}_z^{ref} = M\dot{z}_G^{ref}. \quad (32)$$

From Eq.(2), the reference of ξ_B can be found by the resolved momentum control[7] as

$$\boldsymbol{\xi}_B = \boldsymbol{A}^{-1}\boldsymbol{y}, \quad (33)$$

where

$$\boldsymbol{y} \equiv \begin{bmatrix} \mathcal{P}^{ref} \\ \mathcal{L}^{ref} \end{bmatrix} - \sum_{i=1}^{2}\begin{bmatrix} \boldsymbol{M}_{F_i}^* \\ \boldsymbol{H}_{F_i}^* \end{bmatrix}\boldsymbol{\xi}_{F_i}^{ref} - \sum_{i=1}^{2}\begin{bmatrix} \boldsymbol{M}_{H_i}^* \\ \boldsymbol{H}_{H_i}^* \end{bmatrix}\boldsymbol{\xi}_{H_i}^{ref}, \quad (34)$$

$$\boldsymbol{A} \equiv \begin{bmatrix} \boldsymbol{M}_B^* \\ \boldsymbol{H}_B^* \end{bmatrix}. \quad (35)$$

Finally, the joint velocity of the robot can be obtained by Eqs.(3) and (4). The block diagram of the proposed pattern generator is shown in Fig.2.

E. The Algorithm

A motion pattern of a humanoid robot walking on a rough terrain can be generated by the following algorithm.

Algorithm 1: **Walking Pattern Generation**

1) Give $(\boldsymbol{v}_{F_i}^{ref}, \boldsymbol{\omega}_{F_i}^{ref})$, $(\boldsymbol{v}_{H_i}^{ref}, \boldsymbol{\omega}_{H_i}^{ref})$ and $(\boldsymbol{v}_B^{ref}, \boldsymbol{\omega}_B^{ref})$.
2) Find $(\dot{\boldsymbol{\theta}}_{leg_1}^{ref}, \dot{\boldsymbol{\theta}}_{leg_2}^{ref})$ by Eq.(3) and $(\dot{\boldsymbol{\theta}}_{arm_1}^{ref}, \dot{\boldsymbol{\theta}}_{arm_2}^{ref})$ by Eq.(4) respectively.
3) Find $\mathcal{L}^{ref}$ by Eq.(1) and $\dot{\mathcal{L}}^{ref}$ by differentiation.
4) Give $\ddot{z}_G^{ref}$.
5) Give λ_k^{ref}.
6) Find $\ddot{x}_G^{ref}, \ddot{y}_G^{ref}$ by solving Eqs.(19) and (20).
7) Find $\mathcal{P}^{ref}$ by Eqs.(30), (31) and (32).
8) Find $\boldsymbol{\xi}_B^{ref}$ by Eq.(33).
9) If $\boldsymbol{v}_B^{ref}$ found in Step 8 is close enough to $\boldsymbol{v}_B^{ref}$ given in Step 1, go to Step 10, otherwise let $\boldsymbol{v}_B^{ref}$ be that found in Step 8 and return to Step 1.

10) Find $(\dot{\boldsymbol{\theta}}_{leg_1}, \dot{\boldsymbol{\theta}}_{leg_2})$ by Eq.(3) and $(\boldsymbol{\theta}_{arm_1}, \boldsymbol{\theta}_{arm_2})$ by Eq.(4), and terminate the algorithm.

Step 1-Step 8 are shown in Fig. 2. The iteration is necessary, since $\dot{\mathcal{L}}$ in Step 3 was found from $\boldsymbol{v}_B^{ref}$ before solving Eqs.(19) and (20), and may produce an unnatural motion by Eq.(33). Note that $\boldsymbol{\omega}_B^{ref}$ is not renewed, otherwise the loop will produce the identical motion with the previous iteration.

Algorithm 1 proved that a strongly stable motion pattern of a humanoid robot walking on a rough terrain should exist if the friction force equations have a solution. This is the first rigorous proof that a strongly stable motion of a humanoid robot walking on a rough terrain should exist under the sufficient friction assumption if the friction force equations has a solution.

III. EXAMPLES

Algorithm 1 is implemented for the dynamic model of humanoid robot HRP-2 [9] whose configuration of the joints is shown in Fig.1. Several implementation examples are investigated in the following.

A. Walking on a Horizontal Plane

In the case, $\forall\ k; \boldsymbol{n}_k = (0,0,1)$, and $\forall\ k; z_k = z_0$ where z_0 is the height of the horizontal plane, $\alpha = 0$, and then Eqs.(21)-(23) become

$$y_C = 0, \tag{36}$$

$$z_C = \sum_{k=1}^{K} \frac{\epsilon_k}{\epsilon} z_0 = z_0, \tag{37}$$

$$x_C = 0, \tag{38}$$

and Eqs.(19) and (20) do

$$M(\ddot{z}_G + g) y_G - M\ddot{y}_G(z_G - z_0) + \dot{\mathcal{L}}_x = \sum_{k=1}^{K} \epsilon_k y_k, \tag{39}$$

$$-M(\ddot{z}_G + g) x_G + M\ddot{x}_G(z_G - z_0) + \dot{\mathcal{L}}_y = -\sum_{k=1}^{K} \epsilon_k x_k, \tag{40}$$

which are equivalent to the ZMP equations[5].

In Step 1 of Algorithm 1, $(\boldsymbol{v}_{F_i}^{ref}, \boldsymbol{\omega}_{F_i}^{ref})$ and $(\boldsymbol{v}_{H_i}^{ref}, \boldsymbol{\omega}_{H_i}^{ref})$ are chosen to be smooth curves as well as the initial trajectory of $\boldsymbol{v}_B^{ref}$, and that of $\boldsymbol{\omega}_B^{ref}$ is set zero for the whole period. The trajectory of $(\sum_{k=1}^{K} \epsilon_k y_k, -\sum_{k=1}^{K} \epsilon_k x_k)$ can be planned as described in the previous section. Fig.3 shows the trajectories of the orientation of the waist link about x, y, z-axes for ten walking steps, which was obtained by five iterations of the algorithm. We can observe that the trajectories were converging to zero by the iterations.

Fig.4 shows the trajectories of the ZMP in which that of the dynamics simulation is in the broken curve and that of the experiment in the solid curve. The dynamics simulation was done using OpenHRP[8] and the experiment using HRP-2. The robot walks along x-axis which is the horizontal axis in the figure. The ZMP is drawn to show that it stays in the support polygon of the robot both in the simulation and the experiment.

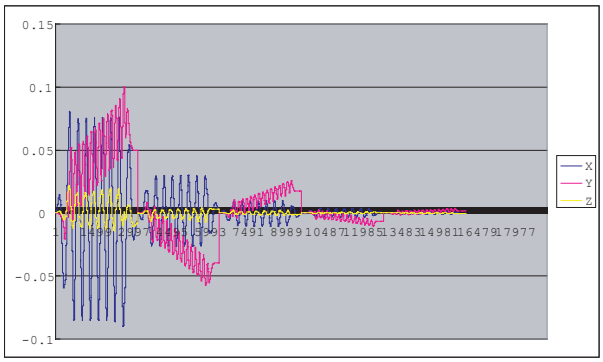

Fig. 3. Trajectories of the orientation of the waist link

B. Walking on Horizontal Steps

In the case, set $\alpha = 0, \forall\ k; \boldsymbol{n}_k = (0,0,1)$, $z_k = z_{F1}, k = 1, \cdots, K_{F1}$ and $z_k = z_{F2}, k = K_{F2}+1, \cdots, K_{F1}+K_{F2}$ where z_{F1} and z_{F2} are the heights of two steps respectively and K_{F1} and K_{F2} are the numbers of the contact points on two steps respectively, and then Eqs.(19)-(20) become

$$M(\ddot{z}_G + g) y_G - M\ddot{y}_G(z_G - z_C) + \dot{\mathcal{L}}_x = \sum_{k=1}^{K} \epsilon_k y_k, \tag{41}$$

$$-M(\ddot{z}_G + g) x_G + M\ddot{x}_G(z_G - z_C) + \dot{\mathcal{L}}_y = -\sum_{k=1}^{K} \epsilon_k x_k, \tag{42}$$

where

$$\begin{aligned} z_C &= z_{F1} \sum_{k=1}^{K_{F1}} \epsilon_k + z_{F2} \sum_{k=K_{F1}+1}^{K_{F1}+K_{F2}} \epsilon_k \\ &= (1-\lambda) z_{F1} + \lambda z_{F2}, \end{aligned}$$

$$0 \le \lambda \le 1.$$

Noting that Eqs.(39) and (40) become identical with Eqs.(41) and (42) by replacing z_0 with z_C, the equations can be interpreted to consider a virtual horizontal plane between consecutive steps and to set the reference ZMP on the plane. The interpretation may be a typical heuristics that has been used to plan motion patterns of a robot that goes up and down stairs, but it has been turned out that the strong stability should be guaranteed in the case by Theorem 1.

C. Walking on a Rough Terrain

This is a generic case, and Eqs.(19)-(20) are used in a generic form. Fig.5 shows an example in which HRP-2 should walk on planes with different slopes and heights. In other words, HRP-2 walks on a rough terrain, but the whole soles of HRP-2 can contact with the terrain in the example. The trajectory of (τ'_{Cx}, τ'_{Cy}) on $f_{Cz} = Mg$ of a walking along x-axis planned by the proposed algorithm is drawn by the red curve in Fig.6, where the horizontal axis is τ'_{Cx} and the vertical axis τ'_{Cy}. The rectangles show the boundary of the CWCs in $f_{Cz}\tau'_{Cx}\tau'_{Cy}$ space corresponding to the single

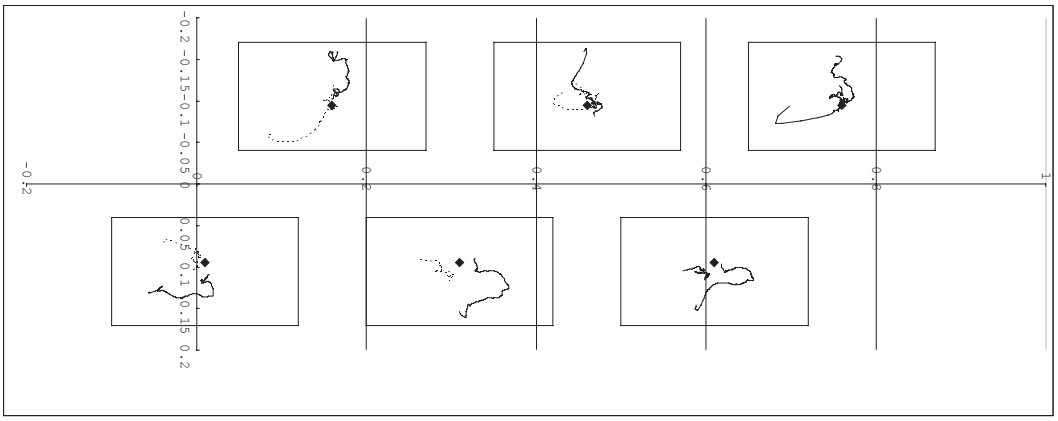

Fig. 4. Trajectories of the ZMP in the simulation and experiment for walking on a horizontal plane

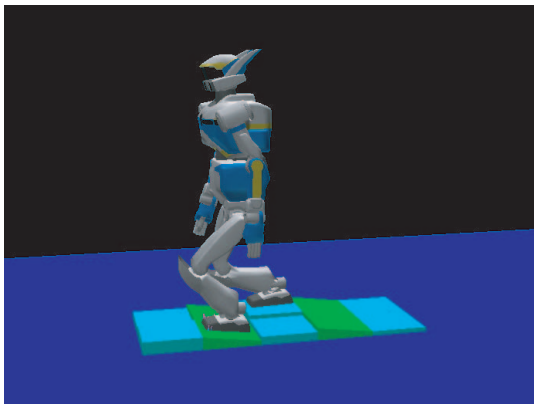

Fig. 5. HRP-2 walking on planes with different slopes and heights

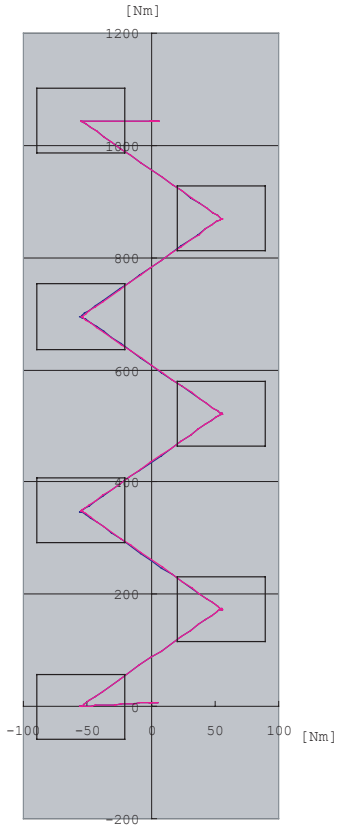

Fig. 6. Trajectories of (τ'_{Cx}, τ'_{Cy}) on $f_{Cz} = Mg$ of walking on planes with different slopes and heights

support phases respectively. It is observed that (τ'_{Cx}, τ'_{Cy}) stay inside the CWCs as planned.

The trajectory of (τ'_{Cx}, τ'_{Cy}) on $f_{Cz} = Mg$ of the walking planned by the ZMP criterion is also drawn by the blue curve in Fig.6 in which the ZMP is defined under the assumption that the floor is a horizontal plane. Two curves almost coincide, because the whole sole of the robot is contact with a slope in a single support phase, the normal vectors of the contact points are identical for each footprint, and then there is not significant difference between the desired (τ'_{Cx}, τ'_{Cy}) derived from two criteria. Fig.7 shows the trajectories of (τ'_{Cx}, τ'_{Cy}) on $f_{Cz} = Mg$ of a single support phase of the walking in the dynamic simulation (left) and the experiment (right) of the planned walking. The trajectories of the other single support phases are similar.

Fig.8 shows an example in which a sole of HRP-2 is contact with the terrain by point contacts for a footprint. Then the normal vectors of the contact points are not identical for the phase. The trajectory of (τ'_{Cx}, τ'_{Cy}) on $f_{Cz} = Mg$ for the single support phase planned by the CWS is drawn by the red curve and that by the ZMP by the blue curve in Fig.9. It is observed that two curves are not coincide in the case, and that the red curve should pass through the center of the CWC. The larger the slope is, more the difference is. Note that the boundary of the CWC is not a rectangle in the case, though that of the support polygon stays to be a rectangle.

Fig.7 shows the trajectories of (τ'_{Cx}, τ'_{Cy}) on $f_{Cz} = Mg$ of the single support phase of the walking in the dynamic simulation (left) and the experiment (right) of the planned walking. It is observed that the curve is close to the boundary, which may be caused by the landing impact force between the foot and the slope of $\frac{1}{6\pi}$ radian.

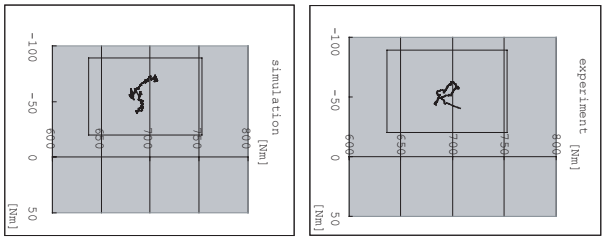

Fig. 7. Trajectories of (τ'_{Cx}, τ'_{Cy}) on $f_{Cz} = Mg$ in the dynamic simulation (left) and the experiment (right) of walking on planes with different slopes and heights

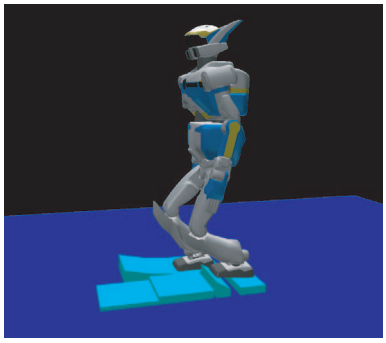

Fig. 8. HRP-2 walking on a rough terrain with point contacts

IV. CONCLUSIONS

The contributions of the paper can be summarized as follows.

- A pattern generator of a humanoid robot that walks on a flat plane, steps and a rough terrain is proposed. It is guaranteed rigorously that the generated pattern should keep the desired contact between the robot and the terrain under the sufficient friction assumption.
- It is shown that there should be a feasible set of friction forces if the friction force equations have a solution.
- The pattern generator is implemented and the verification of the algorithm has been done successfully by the simulations and experiments.

The future works include the experiments using a humanoid robot that has a sensor to find 3-D geometry of the terrain.

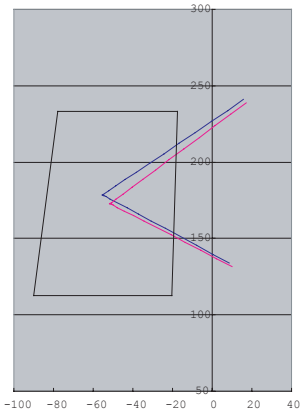

Fig. 9. Trajectories of (τ'_{Cx}, τ'_{Cy}) on $f_{Cz} = Mg$ of walking on a rough terrain with point contacts

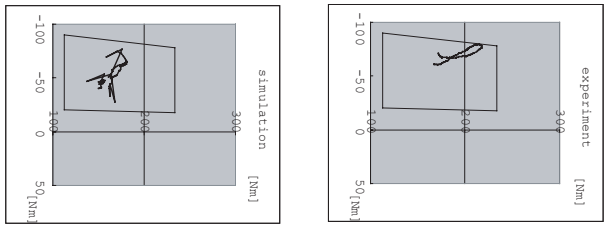

Fig. 10. Trajectories of (τ'_{Cx}, τ'_{Cy}) on $f_{Cz} = Mg$ in the dynamic simulation (left) and the experiment (right) of walking on a rough terrain with point contacts

REFERENCES

[1] D.J.Balkcom and J.C.Trinkle, Computing wrench cones for planar rigid body contact tasks, Int. J. Robotics Research, vol.21, no.12, pp.1053-1066, 2002.

[2] A.J.Goldman and A.W.Tucker, Polyhedral Convex Cones, Annals of Math. Studies, pp.19–40, Princeton, 1956.

[3] A.Goswami, Postural stability of biped robots and the foot rotation indicator (FRI) point, Int. J. Robotics Research, vol.19, no.6, pp.523-533, 1999.

[4] K.Harada, S.Kajita, K.Kaneko, and H.Hirukawa, ZMP Analysis for Arm/Leg Coordination, Proc. IEEE/RSJ Int. Conf. on Intelligent Robots and Systems, Oct.2003.

[5] H.Hirukawa, S.Hattori, K.Harada, S.Kajita, K.Kaneko, F.Kanehiro, K.Fujiwara and M.Morisawa, A Universal Stability Criterion of the Foot Contact of Legged Robots – Adios ZMP, Prof. IEEE International Conference on Robotics and Automation, 2006.

[6] S.Kajita, F. Kanehiro, K. Kaneko, K. Fujiwara, K. Harada, K. Yokoi, H. Hirukawa, Biped Walking Pattern Generation by using Preview Control of Zero-Moment Point, Proc. IEEE International Conference on Robotics and Automation, 2003.

[7] S.Kajita, F.Kanehiro, K.Kaneko, K.Fujiwara, K.Harada, K.Yokoi and H.Hirukawa, Resolved Momentum Control: Humanoid Motion Planning based on the Linear and Angular Momentum, Prof. IEEE International Conference on Intelligent Robots and Systems, 2003.

[8] F.Kanehiro, H.Hirukawa and S.Kajita, OpenHRP: Open Architecture Humanoid Robotics Platform, International Journal of Robotics Research, vol.23, no.2, pp.155–165, 2004.

[9] K.Kaneko, F.Kanehiro, S.Kajita, H.Hirukawa, T.Kawasaki, M.Hirata, K.Akachi and T.Isozumi, Humanoid Robot HRP-2, Prof. IEEE International Conference on Robotics and Automation, 2004.

[10] K.Nishiwaki, S.Kagami, Y.Kuniyoshi, M.Inaba and H.Inoue, Online Generation of Humanoid Walking Motion based on a Fast Generation Method of Motion Pattern that Follows Desired ZMP, Prof. IEEE International Conference on Intelligent Robots and Systems, 2002.

[11] H.O.Lim, Y.Kaneshima, A.Takanishi, Online Walking Pattern Generation for Biped Humanoid Robot with Trunk, Prof. IEEE International Conference on Robotics and Automation, vol.3, pp.3111-3116, 2002.

[12] J.Pang and J.Trinkle, Stability characterizations of rigid body contact problems with Coulomb friction, Zeitschrift fur Angewandte Mathematik und Mechanik, vol.80, no.10, pp.643-663, 2000.

[13] T.Saida, Y.Yokokoji and T.Yoshikawa, FSW (feasible solution of wrench) for Multi-legged Robots, Proc. IEEE Int. Conf. on Robotics and Automation, pp.3815-3820, 2003.

[14] J.Trinkle, J.Pang, S.Sudarsky and G.Lo, On dynamic multi-rigid-body contact problems with Coulomb friction, Zeitshrift fur Angewandte Mathematik und Mechanik, vol.77, no.4, pp.267-279, 1997.

[15] M.Vukobratovic and J.Stepanenko, On the stability of Anthropomorphic Systems, Mathematical Biosciences, vol.15, pp.1-37, 1972.

[16] K.Yoneda and S.Hirose, Tumble Stability Criterion of lntegrated Locomotion and Manipulation, Proc. IEEE/RSJ Int. Conf. on Intelligent Robots and Systems, pp.870-876, 1996.